

Particle entry into the magnetosphere with a southward interplanetary magnetic field studied by a three-dimensional electromagnetic particle code

K.-I. Nishikawa

Department of Physics and Astronomy, Louisiana State University, Baton Rouge

Abstract. We report progress in the long-term effort to represent the interaction of the solar wind with the Earth's magnetosphere using a three-dimensional electromagnetic particle code. A new run that includes an interplanetary magnetic field yields results that are encouragingly consistent with established features of the solar wind-magnetosphere interaction. After a quasi-steady state is established with an unmagnetized solar wind we switch on a southward interplanetary magnetic field (IMF), which causes the magnetosphere to stretch and allows particles to enter the cusps and nightside magnetosphere. Analysis of magnetic fields near the Earth confirms a signature of magnetic reconnection at the dayside magnetopause, and the plasma sheet in the near-Earth magnetotail clearly thins. Later magnetic reconnection also takes place in the near-Earth magnetotail. Arrival of southward IMF near the front of the magnetosphere causes a sunward velocity in the dayside magnetosphere, as required to feed flux tubes into the dayside reconnection process. Sunward flow near the equatorial plane of the magnetosphere implies a dawn-to-dusk electric field. Initially, the velocity in the distant tail is not much affected by the southward turning. Therefore the dawn-dusk electric field increases in the sunward direction, which causes B_z to decrease with time in the near-Earth magnetotail. The cross-field current also thins and intensifies, which excites a kinetic (drift kink) instability along the dawn-dusk direction. As a result of this instability the electron compressibility effect appears to be reduced and to allow the collisionless tearing to grow rapidly with the reduced B_z component. At the same time the nightside magnetic fields are dipolarized and a plasmoid is formed tailward. We find that due to the reconnection particles were injected toward the Earth from the neutral line (X line). Consistent with this dawn-dusk electric field and magnetic reconnection at the dayside magnetopause, both ions and electrons enter the magnetospheric interior easily. In our simulations, kinetic effects self-consistently determine the dissipation rate in the magnetopause associated with reconnection.

1. Introduction

The interaction of the solar wind with the Earth's magnetic field gives rise to a number of important and intriguing phenomena, many of which are only partially understood. These include reconnection between the solar wind magnetic field and geomagnetic field lines at the dayside magnetopause (including flux transfer events), the drag of the solar wind exerted on the magnetotail and associated instabilities at the magnetopause, the plasma convection in the magnetosphere/ionosphere, and the generation of field-aligned current systems. There is a wide range of physical processes involved in the solar wind-magnetosphere system,

and consequently a wide array of methods has been used to study them, ranging from detailed studies of select phenomena with the assumption of a specific field geometry or boundary conditions, to fully three-dimensional simulations with MHD assumptions.

In MHD codes (for example, see *Fedder et al.* [1995]) the microscopic processes can be represented by statistical (macroscopic) constants such as diffusion coefficients, anomalous resistivity, viscosity, temperature, equation of state, and the adiabatic constant. The near-Earth magnetotail is one of the regions where kinetic effects are critical and particle simulations become very important. Two-dimensional local particle simulations show the formation of a thin current sheet a deep minimum in the equatorial B_z field in the near-Earth magnetotail with the inductive electric field carried by a southward interplanetary magnetic field (IMF) [*Pritchett and Coroniti*, 1995]. Recently, three-dimensional particle

Copyright 1997 by the American Geophysical Union.

Paper number 97JA00826.
0148-0227/97/97JA-00826\$09.00

simulations indicate that the collisionless tearing instability grows rapidly as a result of the reduction of electron compressibility caused by the persistent drift kink mode in the presence of a small B_z component [Pritchett and Coroniti, 1996]. Those simulations simulate only the near-Earth region; therefore the resolutions in space and time are better than those in the global simulations [Buneman *et al.*, 1992, 1995]. However, effects from the dayside magnetopause, self-consistent stretched magnetic field by the solar wind with an IMF in the magnetotail, and particle entry from low-latitude boundary layer are not included, which may be important for the magnetotail dynamics (see, for example, Baker *et al.* [1996] and Sergeev *et al.* [1996]).

With the model presented here, we intend to investigate the global simulation of the solar wind interaction with an interplanetary magnetic field using a particle code which contains the complete particle physics. As will be shown below, the advantage is that the basic equations of the model contain the complete physics. The price to be paid is that, with present supercomputers, plasma parameters must be scaled.

2. Three-Dimensional Electromagnetic Particle Simulation Model

Our code is a successor to the TRISTAN code [Buneman *et al.*, 1980]. Its new features [Buneman, 1993] are (1) Poisson's equation and Fourier transforms have been eliminated by updating the fields locally from the curl equations and depositing the particle currents according to charge-conserving formulas [Villasenor and Buneman, 1992], (2) radiating boundary conditions are applied to the fields using a first-order Lindman approximation [Lindman, 1975], (3) filtering is done locally, (4) localization makes the code ideally suited to modern parallel machines which call for minimizing data paths, (5) the code is in FORTRAN and fully transportable: modest versions run on PCs and on workstations. The new version of the code has been applied to the study of the dynamics of low- β plasma clouds [Neubert *et al.*, 1992], the whistler waves driven by the Spacelab 2 electron beam [Nishikawa *et al.*, 1994a; Zhao *et al.*, 1994], and a coalescence of two current loops [Nishikawa *et al.*, 1994b; Zhao *et al.*, 1995, 1996].

For the simulation of solar wind-magnetosphere interactions the following boundary conditions were used for the particles [Buneman *et al.*, 1992, 1995; Nishikawa *et al.*, 1995, also Thinning of near-Earth magnetotail with southward IMF as simulated by a 3-D EM particle code, submitted to *Geophysical Research Letters*, 1996, hereafter referred to as unpublished manuscript, 1996]: (1) Fresh particles representing the incoming solar wind (unmagnetized in our test run) are continuously injected across the yz plane at $x = x_{min}$ with a thermal velocity plus a bulk velocity in the $+x$ direction; (2) thermal solar particle flux is also injected

across the sides of our rectangular computation domain; (3) escaping particles are arrested in a buffer zone, redistributed there more uniformly by making the zone conducting in order to simulate their escape to infinity, and finally written off. We use a simple model for the ionosphere where both electrons and ions are reflected by the Earth's dipole magnetic field. Effects of a conducting ionospheric boundary will be developed in future simulations. The effects of the Earth's rotation are not included.

For the fields, boundary conditions were imposed just outside these zones [Buneman *et al.*, 1992, 1995; Nishikawa *et al.*, 1995, unpublished manuscript, 1996]: radiation is prevented from being reflected back inward, following Lindman's ideas [Lindman, 1975]. The lowest order Lindman approximation was found adequate: radiation at glancing angles was no problem. However, special attention was given to conditions on the edges of the computational box.

In order to bring naturally disparate time scale and space scale closer together in this simulation of phenomena dominated by ion inertia and magnetic field interaction, the natural electron mass was raised to 1/16 of the ion mass and the velocity of light was lowered to twice the incoming solar wind velocity. This means that charge separation and kinetic phenomena are included qualitatively but perhaps not with quantitative accuracy. Likewise, radiation-related phenomena (e.g., whistler modes) are included qualitatively.

3. Simulation Results

A first test exploring the solar wind-magnetosphere interaction was run on the CRAY-YMP at NCAR using a modest 105 by 55 by 55 grid and only 200,000 electron-ion pairs [Buneman *et al.*, 1992]. We also have reported on our second test run on the CRAY-2 at NCSA using a larger 215 by 95 by 95 grid and about 1,500,000 electron-ion pairs [Buneman *et al.*, 1995]. Initially, these fill the entire box uniformly and drift with a velocity $v_{sol} = 0.5c$ in the $+x$ direction, representing the solar wind without an IMF. The electron and ion thermal velocities are $v_{et} = (T_e/m_e)^{1/2} = 0.2c$, and $v_{it} = (T_i/m_i)^{1/2} = 0.05c (= v_s = (T_e/m_i)^{1/2})$, respectively, while the magnetic field is initially zero. A circular current generating the dipole magnetic field is increased smoothly from 0 to a maximum value reached at time step 65 and kept constant at that value for the rest of the simulation. The center of the current loop is located at $(70.5\Delta, 47.5\Delta, 48\Delta)$ with the current in the xy plane and the axis in the z direction. The initial expansion of the magnetic field cavity is found to expel a large fraction of the initial plasma. The injected solar wind density is about 0.8 electron-ion pairs per cell, the mass ratio is $m_i/m_e = 16$, and $\omega_{pe}\Delta t = 0.84$.

The first results that include magnetic reconnection at the dayside magnetopause and thinning of the near-

Earth magnetotail as the effects of an interplanetary magnetic field were reported briefly (Nishikawa et al., unpublished manuscript, 1996). This paper contains further results, including particle entry into the inner magnetosphere and the near-Earth magnetotail, and magnetic reconnection in the near-Earth magnetotail. At step 768 [Buneman et al., 1995; Nishikawa et al., 1995] a southward IMF ($B_z^{IMF} = -0.4$) is switched on, and the southward IMF front reaches about $x = 120\Delta$ at step 1280. The Alfvén velocity with this IMF is $v_A/c = 0.1(\bar{n}_i)^{-1/2} = 0.1$ for the average ion density $\bar{n}_i = 1$.

Plate 1 shows the electron density in the xz plane containing the dipole center at time steps 1280 (Plate 1a) and 1344 (Plate 1b) with the southward IMF. (The time step used in the simulations corresponds to about 4 seconds in nature.) The electron density is color coded and the magnetic field component in the plane is shown

with arrows at every third grid point. The magnitude of the field has been scaled in order to make the field direction clearer for weak fields, so that the length of the vectors is not a true representation of the field magnitude. The plasma flows through the simulation domain from left to right (low to high x -values). In the process, the dipole field is compressed on the side facing the plasma wind and is extended to a long tail on the downwind side, just as the Earth's magnetic field in the solar wind [Buneman et al., 1992, 1995; Nishikawa et al., 1995, unpublished manuscript, 1996]. More particles penetrate into the magnetotail near the Earth in the case of southward IMF, as shown in Plate 1, than in the case without the IMF, as shown by Nishikawa et al. [1995]. This is attributable to magnetic reconnection at the dayside magnetopause [Fu et al., 1995; Swift, 1996, and references therein]. As shown in the previous paper (Nishikawa et al., unpublished manuscript, 1996),

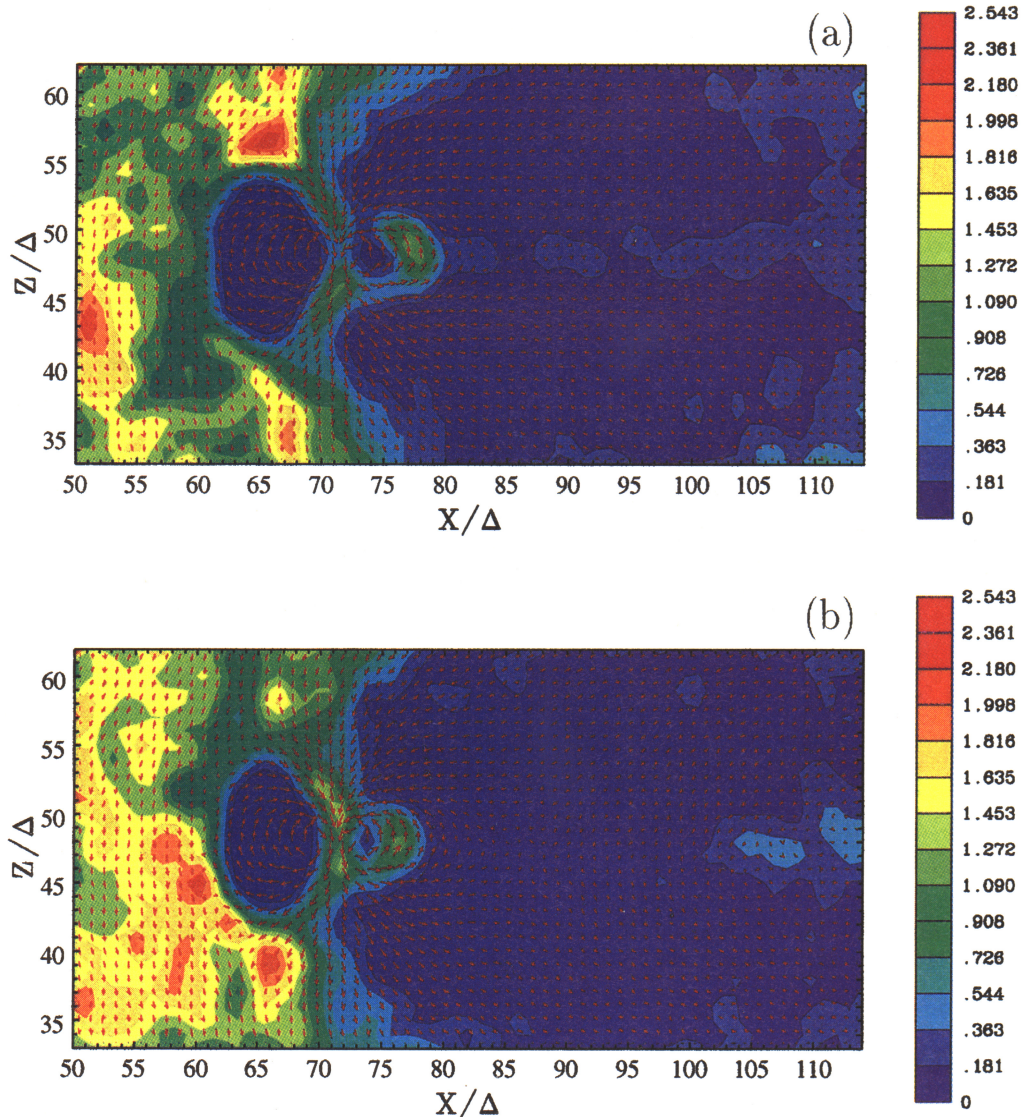


Plate 1. Electron density in the xz plane containing the dipole center at step (a) 1280 and (b) 1344. “Relative amplitude” on color bar signifies simulation units. The arrows show the magnetic fields.

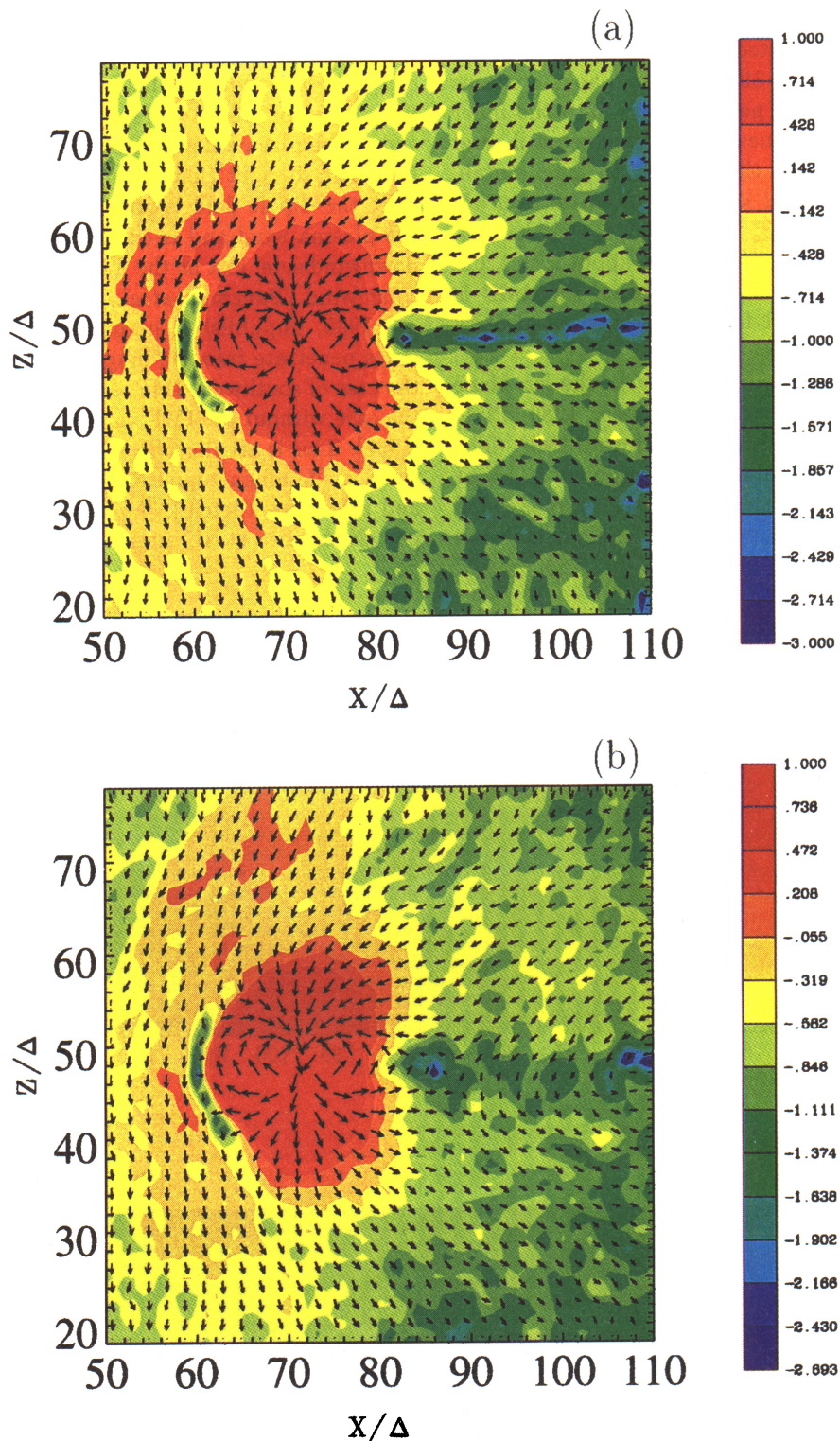


Plate 2. Magnetic field strength in the xz plane containing the dipole center at step (a) 1280 and (b) 1344. The arrows show the magnetic field.

at time step 1216 the near-Earth magnetotail clearly thins [see Nishikawa et al., unpublished manuscript, 1996, Figure 3b] and a tearing instability starts to grow near $x = 85\Delta (\approx -15R_E)$, and the density is bunched in the magnetotail owing to this instability as shown in Plate 1a. At time step 1344 (Plate 1b) electrons are

evacuated from the X line because of reconnection as found in the previous simulation [Pritchett and Coroniti, 1996]. Some electrons are trapped in the magnetic island (plasmoid) around $x = 108\Delta$ (see Figure 1d).

To display magnetic reconnection at the dayside magnetopause and in the magnetotail, Figure 1 shows the

magnetic field lines in the noon-midnight meridian plane for four different times. (Geocentric solar magnetospheric (GSM) coordinates are used in only Figure 1.) At time step 1024, the solar wind with the southward IMF starts to interact with the dipole magnetic field at the dayside magnetopause (Figure 1a). Figure 1b shows the X point (X line) at the magnetopause (time step 1088) [Swift, 1996]. The southward IMF is bent by the magnetosphere as shown in Figure 1c (time step 1216). Figure 1c, which corresponds to time step 1216, displays an interesting magnetic structure near the subsolar magnetopause. Three-dimensional analysis shows that the reconnection occurs three-dimensionally in the dayside magnetopause along the equator (see, for example, Walker and Ogino [1996]). At the same time the stretched dipole magnetic fields are observed particularly in Figure 1c. Furthermore, the magnetic fields are stretched in the magnetotail, which leads to growth of a tearing instability there. Figure 1d shows magnetic reconnection occurring at time step 1280, with the X point (X line) located near $x = 85\Delta$ (about $-15R_E$) [Pritchett and Coroniti, 1996].

Total magnetic fields $|\mathbf{B}|$ in the noon-midnight cross section as in Figure 1 are plotted in Plate 2 for the time steps 1280 (Plate 2a) and 1344 (Plate 2b). In these figures the maximum and minimum values are set in order to highlight the changes due to reconnection and the thinning of the magnetotail. Plate 2a shows the solar

wind with southward IMF passing the magnetotail (see also Figure. 1d). At time 1280, weak magnetic fields are found at the dayside magnetopause owing to magnetic reconnection (see also Figure 1d). The region with weaker magnetic fields in the magnetotail is very narrow in the z direction, which leads to a tearing instability. At the later time step (1344) the narrowed cross-field current is relaxed as shown in Plate 2b [Pritchett and Coroniti, 1996].

The enhanced near-Earth cross-field current density [Pritchett and Coroniti, 1995] also occurs at this time, as Lui [1991, 1996] has suggested, which may lead to the current disruption. Plate 3 shows that the cross-field current in the near-Earth tail ($85 < x/\Delta < 90$) is about 4 times more intense at time step 1280 (Plate 3b), under the full influence of southward IMF, than at time step 768 (Plate 3a), which corresponds to zero IMF (the scale is different). We infer that the weak B_z field and an anomalous resistivity due to the kinetic (drift kink) instability (current disruption) [Lui, 1991, 1996] may excite the tearing instability [Pritchett and Coroniti, 1996].

The magnetic reconnection takes place around $x = 85\Delta$ (see Figure 1d). The tearing instability is excited by the combined effects of the reduced B_z and the kinetic (drift kink) instability. In order to make sure that the kinetic instability is excited along the y (dawn-dusk) direction, we check the time evolution of the plasma

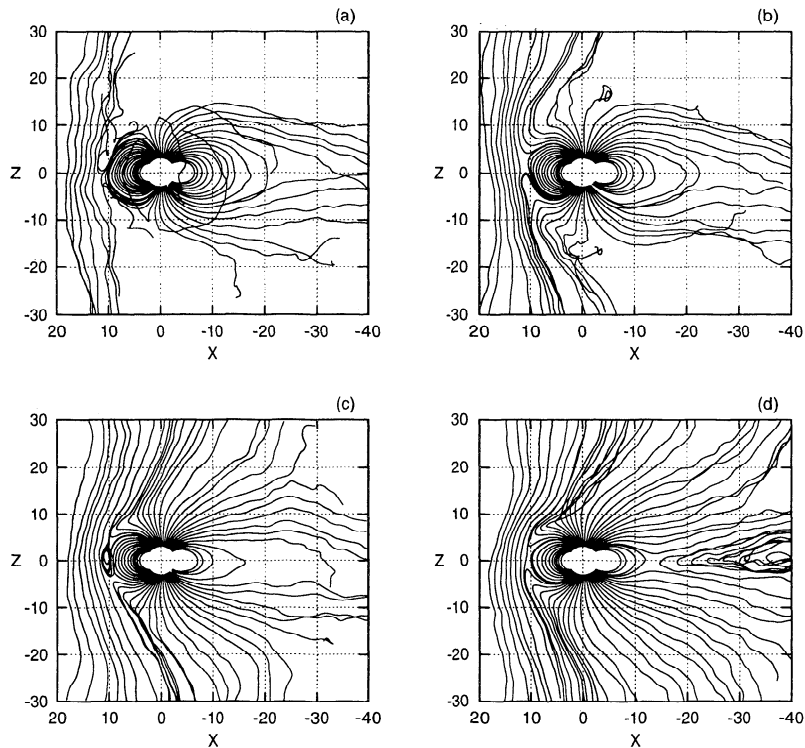


Figure 1. Magnetic field lines in the xz plane containing the dipole center at step (a) 1024, (b) 1088, (c) 1216, and (d) 1280. The magnetic field lines are traced from near the Earth ($r = 3\Delta$ ($\approx 3R_E$)) and subsolar line in the dayside and the magnetotail. Some magnetic field lines are moved toward dawn or duskward. The tracing was terminated due to the preset number of points or the minimum strength of total magnetic field.

sheet in the dawn-dusk cross section at $x = 85\Delta$. The plasma sheet is kinked as shown in the previous localized three-dimensional simulations [Zhu and Winglee, 1996; Pritchett and Coroniti, 1996]. The electron compressibility effect appears to be decreased because of the transport of plasma across flux tubes caused by the drift kink (Alfvén) instability [Pritchett and Coroniti, 1996]. Consequently, the tearing instability grows rapidly. The northward closed magnetic field (see Figure 1c) is disturbed by the drift kink instability. Finally, the X line is created at $x = 82\Delta$ and the plasmoid is formed tailward (see, for example, Birn *et al.* [1996] Walker and Ogino [1996]). Therefore the magnetic field at $x = 85\Delta$ is reversed to southward at time step 1280. At the same time due to the reconnection the electrons are pushed away from the X line region as shown in Plate 1b.

Plate 4 shows the ion density in the equatorial plane of the magnetosphere at time steps 768 (Plate 4a) and 1280 (Plate 4b). As shown in Plate 4b, reconnection at the dayside magnetopause and in the near-Earth magnetotail apparently results in increased ion population in the inner plasma sheet. At the same time, energetic ions (and electrons) are injected into the polar cusps around $x = 72\Delta$, $y = 48\Delta$. These particles are accelerated at the magnetopause by the reconnection electric field. Some particles may be ejected by the formation of the X line because of the tearing instability.

To investigate the increased particle population in the inner plasma sheet, we labeled the particles that lay in the box ($80 \leq x/\Delta \leq 110$, $40 \leq y/\Delta \leq 56$, $40 \leq z/\Delta \leq 56$) at time step 1344 and traced them in time to step 1216. Plate 5 shows the projections of ions (Plate 5a, 5c, and 5e) and electrons (Plate 5b, 5d, and 5f) on the xz , xy , and yz planes. (Particles at time step 1344 and 1216 are plotted in black and red, respectively.) As shown in Plate 5a, 5c, and 5e, ions drift inward from the low-latitude boundary layers and the mantle. As shown in Plate 5c and 5e, more ions drift into the region from the dawnside, while more electrons drift into the region from the dusk side as shown in Plate 5d and 5f. Few electrons came from further down the magnetotail (Figs. 6b and 6d). These particle drifts are consistent with the dawn-dusk electric field brought by the southward IMF.

Plate 6 displays results of a similar particle-traceback from the inner magnetosphere. In order to check immediate effects of the magnetic reconnection at the magnetopause and in the near-Earth magnetotail, we have investigated where particles come from into the inner magnetosphere ($\leq 6\Delta$ ($\approx 6R_E$)) at time step 1344. As in Plate 5, Plate 6 shows the projections of ions (Plate 6a, 6c, and 6e) and electrons (Plate 6b, 6d, and 6f) on the xz , xy , and yz planes. (Particles at time step 1344 and 1216 are plotted in black and red, respectively.) Mainly both ions and electrons come from the nearby magnetosphere. However, some ions move in from the dayside (toward dawn) magnetopause as shown in Plate

6a, 6c, and 6e, while electrons drift from the afternoon side magnetopause. This tendency is consistent with the drifts shown in Plate 5. As shown in Plate 6, the magnetic reconnection occurring at the dayside magnetopause affects strong and rapid particle entry into the inner magnetosphere. It is clearly necessary to trace particles to investigate more precise particle dynamics. These self-consistent particle dynamics can be studied only by particle simulations.

4. Discussion

The results presented in Plates 1 through 6 and Figure 1 show that even with the modest grid size of 215 by 95 by 95 cells, our three-dimensional fully kinetic model is able to generate the complete magnetosphere with some of the basic characteristics observed for southward IMF. For southward IMF, the simulation results show reconnection taking place at the dayside magnetopause and increased particle entry into the magnetosphere. The structure, motion, and occurrence of magnetic reconnection at the dayside magnetopause have been observed [e.g., Phan and Paschmann, 1996; Phan *et al.*, 1996]. Phan and Paschmann [1996] observed that the normal velocity v_n is nearly constant through the magnetopause (as shown in Plate 6). In the case of southward IMF since both \mathbf{E} and \mathbf{B} fields reverse, $\mathbf{E} \times \mathbf{B}$ will not reverse in the dayside magnetopause, which is consistent with the observations. Therefore this reversed \mathbf{E} field through the magnetopause current leads to nonzero $\nabla \times \mathbf{E}$. Investigation of this structure ($\nabla \times \mathbf{E} \neq 0$) and its effects on particle diffusion (due to reconnections) requires further diagnosis, perhaps and improved simulations with better resolutions in space and time.

Southward IMF also causes magnetic field stretching in the near-Earth plasma sheet. The cross-field current also thins and intensifies, which excites a kinetic (drift kink) instability along the dawn-dusk direction. It should be noted that theoretical analysis [Lembège and Pellat, 1982; Pellat *et al.*, 1991; Brittnacher *et al.*, 1994] and particle simulations [Pritchett, 1994; Pritchett and Büchner, 1995] indicate that the collisionless tearing is stabilized by the electron compressibility which results from the finite normal magnetic component (B_z) in the central plasma sheet. The reduced B_z with a kinetic (drift kink) instability in the central plasma sheet apparently allows the collisionless tearing to grow [Pritchett and Coroniti, 1996]. Namely, the plasma transport across tubes caused by the kinetic (drift kink) instability appears to reduce the electron compressibility effect and to allow the collisionless tearing instability grow rapidly. Because of this collisionless tearing instability magnetic reconnection (X line) is formed in the near-Earth magnetotail. At the same time, the nightside magnetic fields are dipolarized and a plasmoid is formed tailward (see, for example, Birn *et al.* [1996] and Walker and Ogino [1996]). A thin, intense current sheet is disrupted, which is observed dur-

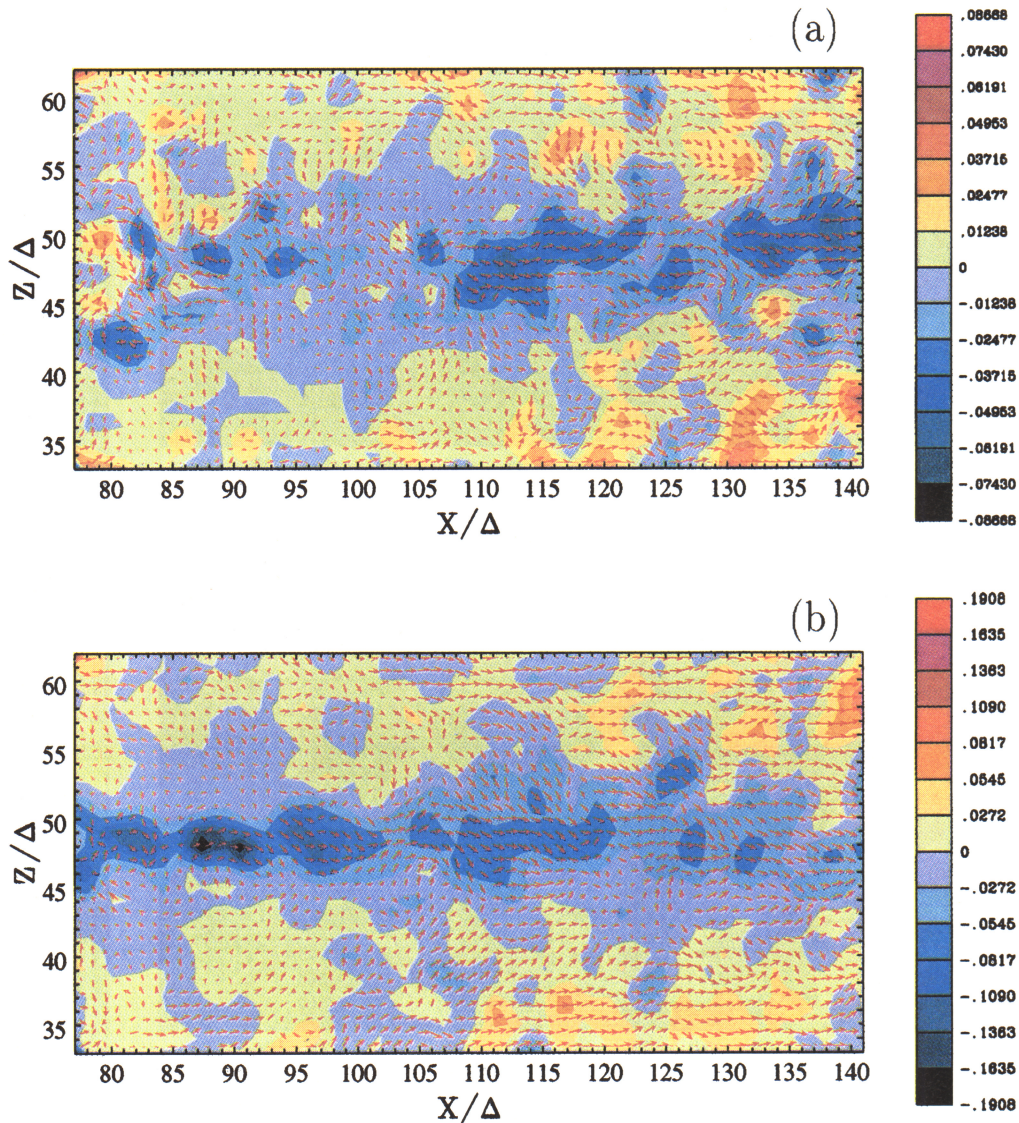


Plate 3. Current density (J_y) in the xz plane at $y = 48\Delta$ at step (a) 768 and (b) 1280. The arrows show the electron flux.

ing substorm breakup and expansion [Lui, 1991, 1996]. In this set of simulations, a southward IMF is switched on after a quasi-steady state with an unmagnetized solar wind. In order to simulate a typical substorm condition, a southward IMF should be switched on after a northward IMF sets the magnetotail and a northward IMF should be switched on. In this way, a more clear substorm will be triggered (see, for example, Baker *et al.* [1996] and Sergeev *et al.* [1996]).

The results reported here suggest that full three-

dimensional electromagnetic particle simulations will become an important tool for the theoretical understanding of Earth's magnetosphere in the not-so-distant future. It is clearly necessary to use more realistic values of m_i/m_e with a larger system and more particles in a cell, which relies on the development of future more powerful and faster supercomputers. This would help to establish more precisely the nature of the magnetic reconnection and associated phenomena and to clarify their relation to the observations. For

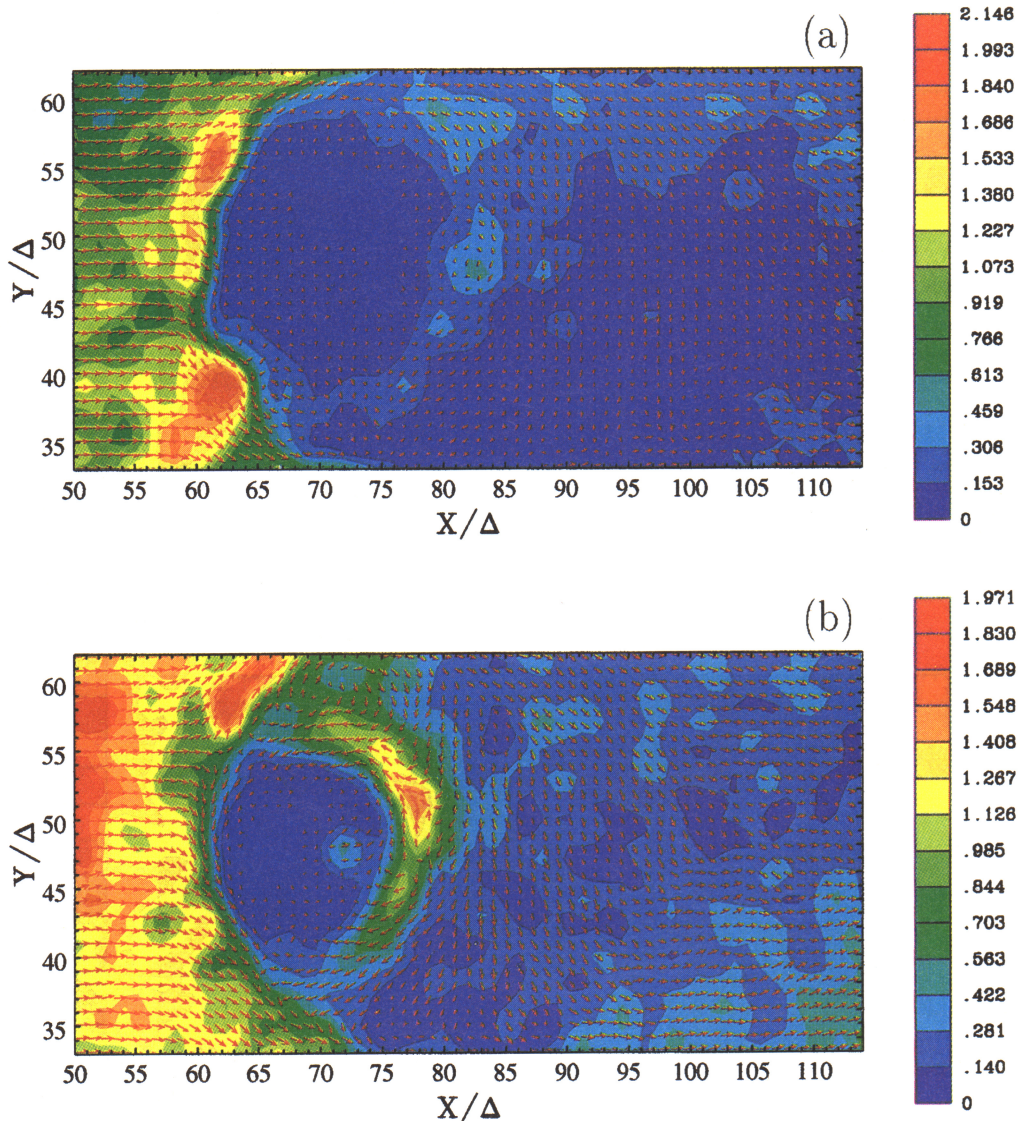


Plate 4. Ion density in the xy plane at $z = 48\Delta$ at step (a) 768 and (b) 1280. The arrows show the ion flux.

the present, however, scaling and grid size remain substantial problems. For example, in our simulation, the Debye length and the thickness of the bow shock are both of the order of an Earth radius, which is of the order of a grid spacing. However, some form of scaling is usually needed in particle simulations, even in one and two dimensions, and still such simulations are able to reveal much of the physics behind natural phenomena. Further simulations including time-dependent IMFs (including B_x , B_y) and transient shocks are in progress and will be reported elsewhere.

Acknowledgments. We thank T. W. Hill, R. A. Wolf, C. Ding, D. Cai, H. Okuda, A. T. Y. Lui, F. R. Toffoletto, and J. Büchner for useful discussions. Support for this work was provided by NSF grants ATM-9106639, ATM-9121116, and ATM-9122310. The development of the simulation code was performed at the National Center for Supercomputing Applications, University of Illinois at Urbana-Champaign and the production runs were performed at Pittsburgh Supercomputing Center. Both centers are supported by the National Science Foundation.

The Editor thanks W. Heikkila and another referee for assistance in evaluating this paper.

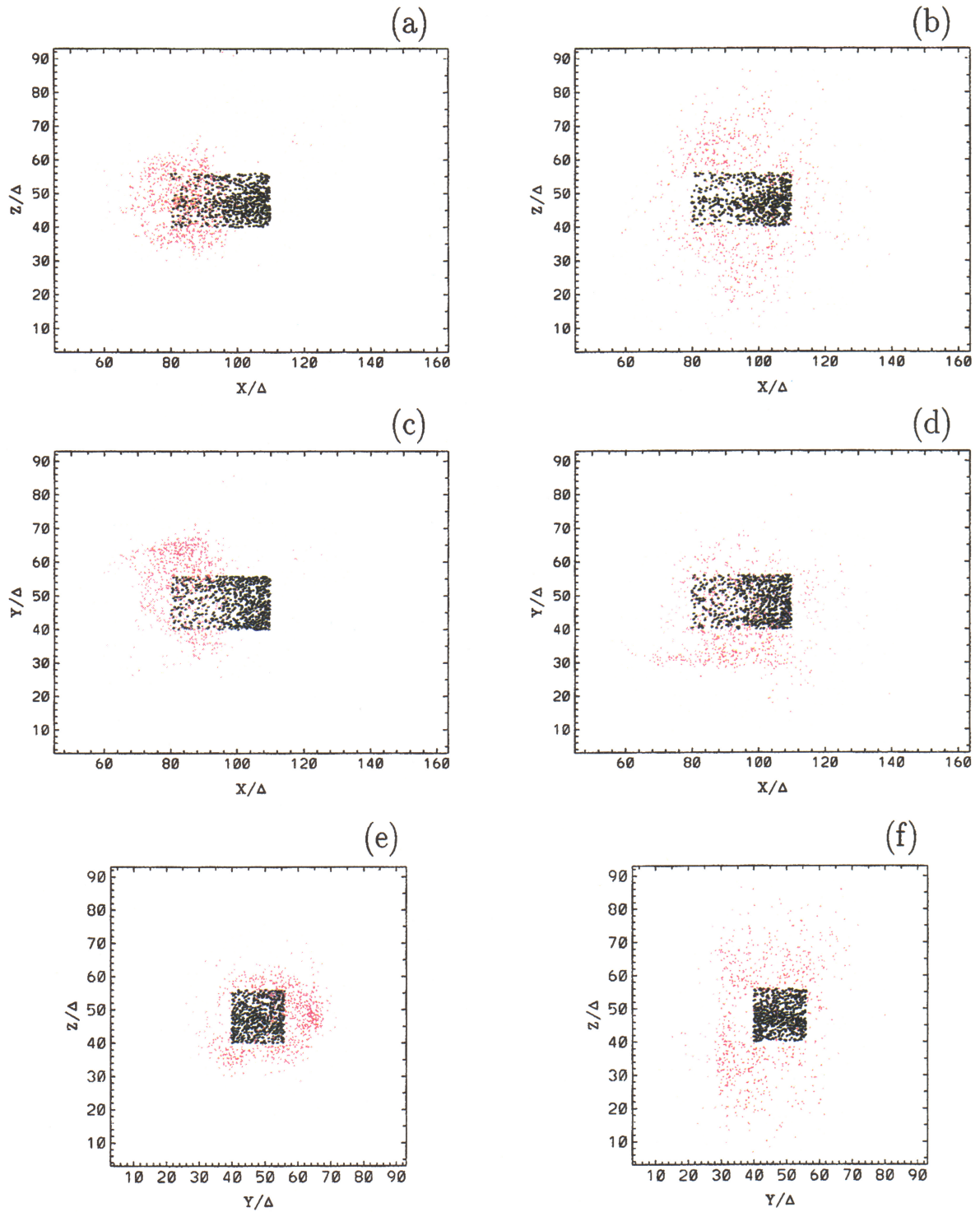


Plate 5. Particle dynamics is checked by tracing. Projections of ions (a, c, and e) and electrons (b, d, and f) are plotted at time step 1216 (red) and 1344 (black) (particles in the box-shaped region ($80 \leq x/\Delta \leq 110$, $40 \leq y/\Delta \leq 56$, $40 \leq z/\Delta \leq 56$)) on the xz (Plate 5a and 5b), xy (Plate 5c and 5d), and yz planes (Plate 5e and 5f).

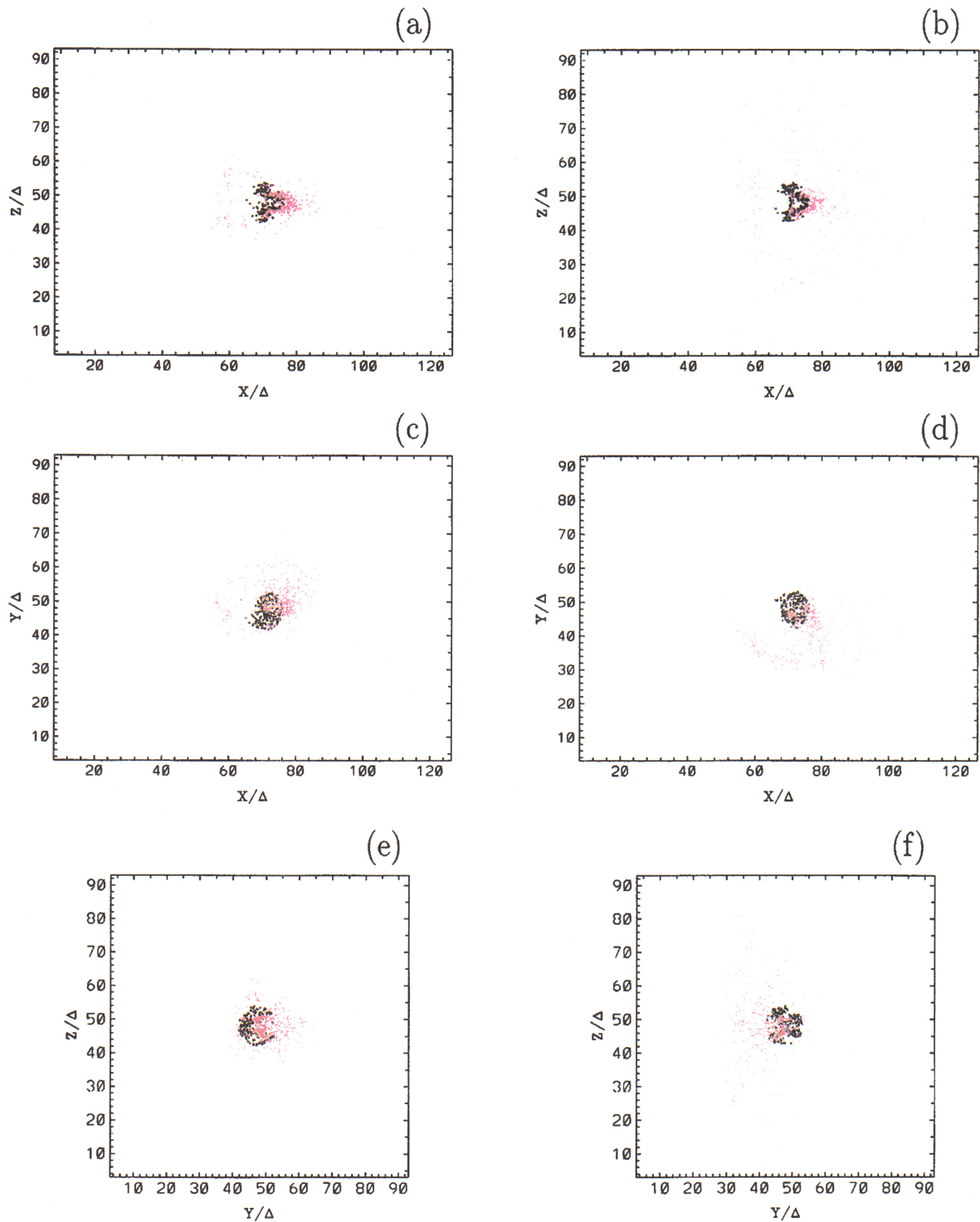


Plate 6. Particle dynamics is checked by tracing. Projections of ions (a, c, and e) and electrons (b, d, and f) are plotted at time step 1216 (red) and 1344 (black) (particles in the sphere-shaped region $((x - 70.5)^2 + (y - 47.5)^2 + (z - 48)^2 \leq 36\Delta^2)$ on the xz (Plate 6a and 6b), xy (Plate 6c and 6d), and yz planes (Plate 6e and 6f).

References

- Baker, D. N., T. I. Pulkkinen, V. Angelopoulos, W. Baumjohann, and R. L. McPherron, Neutral line model of substorms: Past results and present view, *J. Geophys. Res.*, **101**, 12,975, 1996.
- Birn, J., M. Hesse, and K. Schindler, MHD simulation of magnetotail dynamics, *J. Geophys. Res.*, **101**, 12,939, 1996.
- Brittnacher, G. R., K. B. Quest, and H. Karimabadi, On the energy principle and ion tearing in the magnetotail, *Geophys. Res. Lett.*, **21**, 1591, 1994.
- Buneman, O., TRISTAN: The 3-D, E-M particle code, in *Computer Space Plasma Physics, Simulation Techniques and Software*, edited by H. Matsumoto and Y. Omura, p. 67, Terra Sci., Tokyo, 1993.
- Buneman, O., C. W. Barnes, J. C. Green, and D. E. Nielsen, Review: Principles and capabilities of 3-d, E-M particle simulations, *J. Comput. Phys.*, **38**, 1, 1980.
- Buneman, O., T. Neubert, and K.-I. Nishikawa, Solar wind-magnetosphere interaction as simulated by a 3D, EM particle code, *IEEE Trans. Plasma Sci.*, **20**, 810, 1992.
- Buneman, O., K.-I. Nishikawa, and T. Neubert, Solar wind-magnetosphere interaction as simulated by a 3D EM particle code, *Space Plasmas: Coupling Between Small and Medium Scale Processes*, Geophys. Monogr. Ser., vol. 86, edited by M. Ashour-Abdalla, T. Chang, and P. Duscember, p. 347, AGU, Washington, D.C., 1995.
- Fedder, J. A., S. P. Slinker, J. G. Lyon, and R. D. Elphinstone, Global numerical simulation of the growth phase and the expansion onset for a substorm observed by Viking, *J. Geophys. Res.*, **100**, 19,083, 1995.
- Fu, S. Y., Z. Y. Pu, Z. X. Liu, and Q. G. Zong, Simulation study on stochastic reconnection at the magnetopause, *J. Geophys. Res.*, **100**, 12,001, 1995.
- Lembège, B., and R. Pellat, Stability of a thick two-dimensional quasineutral sheet, *Phys. Fluids*, **25**, 1995, 1982.
- Lindman, E. L., Free-space boundary conditions for the time dependent wave equation, *J. Comp. Phys.*, **18**, 66, 1975.
- Lui, A. T. Y., A synthesis of magnetospheric substorm models, *J. Geophys. Res.*, **96**, 1849, 1991.
- Lui, A. T. Y., Current disruption in the Earth's magnetosphere: Observations and models, *J. Geophys. Res.*, **101**, 13,067, 1996.
- Neubert, T., R. H. Miller, O. Buneman, and K.-I. Nishikawa, The dynamics of low- β plasma clouds as simulated by a 3-dimensional, electromagnetic particle code, *J. Geophys. Res.*, **97**, 12,057, 1992.
- Nishikawa, K.-I., O. Buneman, and T. Neubert, Solar Wind-Magnetosphere Interaction as Simulated by a 3-D EM Particle Code, *Astrophys. Space Sci.*, **227**, 265, 1995, also in *Plasma Astrophysics and Cosmology*, edited by A.T. Peratt, p. 265, Kluwer Academic Pub., Norwell, Mass., 1995.
- Nishikawa, K.-I., O. Buneman, and T. Neubert, New aspects of whistler waves driven by an electron beam studied by a 3-D electromagnetic code, *Geophys. Res. Lett.*, **21**, 1019, 1994a.
- Nishikawa, K.-I., J.-I. Sakai, J. Zhao, T. Neubert, and O. Buneman, Coalescence of two current loops with kink instability simulated by 3-D EM particle code, *Astrophys. J.*, **434**, 363, 1994b.
- Pellat, R., F. V. Coroniti, and P. L. Pritchett, Does ion tearing exist?, *Geophys. Res. Lett.*, **18**, 143, 1991.
- Phan, T. D., and G. Paschmann, Low-latitude dayside magnetopause and boundary layer for high magnetic shear, 1, Structure and motion, *J. Geophys. Res.*, **101**, 7801, 1996.
- Phan, T. D., G. Paschmann, and B. U. Ö. Sonnerup, Low-latitude dayside magnetopause and boundary layer for high magnetic shear, 2, Occurrence of magnetic reconnection, *J. Geophys. Res.*, **101**, 7817, 1996.
- Pritchett, P. L., Effect of electron dynamics on collisionless reconnection in two-dimensional magnetotail equilibria, *J. Geophys. Res.*, **99**, 5935, 1994.
- Pritchett, P. L., and J. Büchner, Collisionless reconnection with a minimum in the equatorial magnetic field and with magnetic shear, *J. Geophys. Res.*, **100**, 3601, 1995.
- Pritchett, P. L., and F. V. Coroniti, Formation of thin current sheets during plasma sheet convection, *J. Geophys. Res.*, **100**, 23,551, 1995.
- Pritchett, P. L., and F. V. Coroniti, The role of the drift kink modes in destabilizing thin current sheets, *J. Geomagn. Geoelectr.*, **48**, 833, 1996.
- Sergeev, V. A., T. I. Pulkkinen, and R. J. Pellinen, Coupled-mode scenario for the magnetospheric dynamics, *J. Geophys. Res.*, **101**, 13,047, 1996.
- Swift, D. W., Use of a hybrid code for global-scale plasma simulation, *J. Comput. Phys.*, **126**, 109, 1996.
- Villasenor, J., and O. Buneman, Rigorous charge conservation for local electromagnetic field solvers, *Comp. Phys. Commun.*, **69**, 306, 1992.
- Walker, R. J., and T. Ogino, A global magnetohydrodynamic simulation of the origin and evolution of magnetic flux ropes in the Magnetotail, *J. Geomagn. Geoelectr.*, **48**, 765, 1996.
- Zhao, J., J. I. Sakai, K.-I. Nishikawa, and T. Neubert, Relativistic particle acceleration in an electron-positron plasma with a relativistic electron beam, *Phys. Plasmas*, **1**, 4114, 1994.
- Zhao, J., J. I. Sakai, and K.-I. Nishikawa, Particle simulation on collision between a plasma cloud and a current loop, *Astrophys. J. Lett.*, **449**, L-161, 1995.
- Zhao, J., J. I. Sakai, and K.-I. Nishikawa, Coalescence of two parallel current loops in a non-relativistic electron-positron plasma, *Phys. Plasmas*, **3**, 844, 1996.
- Zhu, Z., and R. M. Winglee, Tearing instability, flux ropes, and the kinetic current sheet kink instability in the Earth's magnetotail: A three-dimensional perspective from particle simulations, *J. Geophys. Res.*, **101**, 4885, 1996.

K.-I. Nishikawa, Department of Physics and Astronomy, Louisiana State University, Baton Rouge, LA 70803 (e-mail: kenichi@rouge.phys.lsu.edu)

(Received July 19, 1996; revised February 10, 1997; accepted March 5, 1997.)